A Perceptually Motivated Active Noise Control Design and Its Psychoacoustic Analysis

Hua Bao and Issa M.S. Panahi

The active noise control (ANC) technique attenuates acoustic noise in a flexible and effective way. Traditional ANC design aims to minimize the residual noise energy, which is indiscriminative in the frequency domain. However, human hearing perception exhibits selective sensitivity for different frequency ranges. In this paper, we aim to improve the noise attenuation performance in perceptual perspective by incorporating noise weighting into ANC design. We also introduce psychoacoustic analysis to evaluate the sound quality of the residual noise by using a predictive pleasantness model, which combines four psychoacoustic parameters: loudness, sharpness, roughness, and tonality. Simulations on synthetic random noise and realistic noise show that our method improves the sound quality and that ITU-R 468 noise weighting even performs better than A-weighting.

Keywords: Active noise control, acoustic noise, human hearing perception, A-weighting, ITU-R 468 noise weighting, psychoacoustics.

I. Introduction

The active noise control (ANC) [1] technique is based on the principle of superposition by generating an appropriate anti-noise, which is a signal with equal amplitude and opposite phase of the primary noise in the ideal situation. The anti-noise is controlled by the adaptive filter [2] in the digital domain. In the realistic system, the noise signal cannot be canceled out completely, which leads to the existence of residual noise. However, regarding mean square error (MSE), the adaptive filter can minimize the residual noise by updating the filter coefficients, which controls the anti-noise signal.

Interest in the research of human factors has grown in engineering [3]. Such research focuses on the idea that objects and machines are built to serve humans and must always be designed with human users in mind. Regarding the ANC technique, it should be noted that the ultimate goal of ANC is to minimize the annoyance of acoustic noise to human hearing. Hence, human hearing sensation is an important factor to be taken into account in the ANC system design. However, the human hearing system has very complicated characteristics. Nonuniform frequency response is one of the most significant features. Psychoacoustic research reveals that the human ear is more sensitive to the mid frequencies than to the very low or very high frequencies. Fletcher and Munson quantified human hearing sensitivity with respect to frequency for single tone sound in the form of equal-loudness contour in 1933 [4].

To obtain a subjectively valid measurement of noise, noise weighting, an amplitude-frequency function, is commonly used to incorporate a nonuniform frequency response. There are two popular noise weighting standards: A-weighting [5] and ITU-R 468 noise weighting [6]. A-weighting was derived from equal-loudness contour for low-level pure tone noise.

Manuscript received Dec. 4, 2012; revised Feb. 9, 2013; accepted Feb. 16, 2013.

Hua Bao (phone: +1 732 888 4249, hua.bao@broadcom.com) is with Mobile and Wireless Group, Broadcom Corporation, New Jersey, USA.

Issa M.S. Panahi (issa.panahi@utdallas.edu) is with the Department of Electrical Engineering, University of Texas at Dallas, Texas, USA.

http://dx.doi.org/10.4218/etrij.13.0112.0822

ITU-R 468 noise weighting was presented by Comité Consultatif International pour la Radio (CCIR) to measure random noise. It is commonly used in Europe. In this paper, noise weighting will be incorporated into the ANC system to improve the perceptual performance. Noise weightings are easy to implement in linear time-invariant (LTI) form. Digital filters can be designed according to the standard amplitude-frequency curves.

By incorporating noise weighting into the ANC system, we present a perceptually motivated ANC system based on the filtered-E least mean square (FELMS) structure initially proposed by Kuo and Tsai [7]. Kuo and Tsai presented FELMS as a method to shape the residual noise spectrum. Although they indicated that human hearing response could be applied, no further investigation has been found. In this paper, we will provide a practical implementation to improve the ANC performance in terms of human perception. We refer to our ANC design, which considers psychoacoustic factors, as psychoacoustic ANC (PANC). In our previous work, the application of A-weighting on ANC was investigated [8], and a delay-less subband structure [9] was utilized to further improve the perceptual performance and computational complexity [10].

Since the target of the PANC system is to minimize the perceptual annoyance of residual noise on human hearing, perceptual measurement should be utilized for performance evaluation. Sound pressure level (SPL), most commonly used for the traditional ANC system, is not a good candidate because it treats the whole frequency range indiscriminately. In [8], [10], noise attenuation performance was evaluated with loudness measurement, which is a psychoacoustic metric for sound intensity. Loudness is one aspect of human sensation. To estimate the overall pleasantness/annoyance of noise, sound quality is considered in this paper. Sound quality research aims to predict human preference for sound [11], [12]. Aures [13] presented an empirical model, which predicted the pleasantness of a sound. This model combines four psychoacoustic measurements: loudness, sharpness, roughness, and tonality [4]. This model has been used for different applications, such as ANC on car noise [14], speech enhancement [15], and so on. In our early attempt [16], we applied sound quality analysis on the PANC system with ITU-R 468 noise weighting in a brief manner. In this paper, we will systematically compare the PANC system with two different noise weightings for both synthetic random noise and realistic environmental noise. Analysis will be conducted to examine the impact of noise weightings on the spectrum of residual noises. The detailed procedure to design the digital filter for noise weightings will also be introduced.

The rest of this paper is organized as follows. Section II briefly reviews the traditional ANC system based on the filtered-X least mean square (FXLMS) structure and delineates the proposed PANC system with noise weighting. Section III explains the psychoacoustic models for loudness, sharpness, roughness, and tonality. The pleasantness model is finally given by combining the above four models. In section IV, we show the simulation results for synthetic random noise and realistic magnetic resonance imaging (MRI) acoustic noises. Finally, conclusions and future work are discussed in section V.

II. Methods

1. Conventional ANC System

In general, the ANC systems can be categorized as feedforward structures or feedback structures [1], [17], [18]. FXLMS is a typical feedforward structure, as shown in Fig. 1. The primary path transfer function, $P(z)$, models the system response from the reference sensor measuring the source noise signal, $x(n)$, to the error sensor measuring the attenuated signal, $e(n)$, at the canceling point. The secondary path transfer function, $S(z)$, respresents the system response from the output of the adaptive filter to the canceling point. $\hat{S}(z)$ is the estimated version of $S(z)$. The FXLMS structure is very tolerant of the estimation error in $\hat{S}(z)$, which can be estimated either online or offline. The "adaptive algorithm" module represents the algorithm that is used to update the coefficients of adaptive filter $W(z)$. Popular adaptive algorithms include the LMS method, the normalized LMS (NLMS) method, recursive least square method, and affine projection algorithm. Once the ANC system begins working, the output of $W(z)$ drives the loudspeaker to send a canceling signal to attenuate the noise in the expected area. The coefficients of $W(z)$ are then updated so that the residual noise is minimized in terms of MSE.

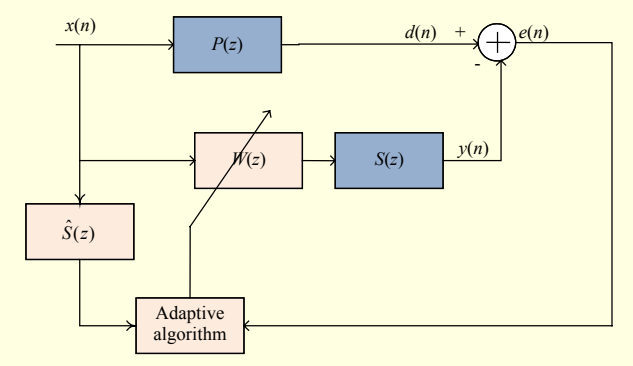

Fig. 1. Conventional ANC system based on feedforward FXLMS.

2. Noise Weighting

Noise weighting is proposed for the purpose of quantifying human hearing sensitivity with respect to frequency. The American National Standards Institute (ANSI) specifies several noise weighting standards: A, B, C, and D. B-weighting, originally intended to represent human response to moderate intensity of sound, is rarely used. C-weighting weights frequencies almost equally. D-weightings (more than one) were designed primarily to measure aircraft noise but have yet to gain complete universal acceptance and are currently used only for very specific measurement applications. Among the four weighting standards, A-weighting is most commonly used. The United States Department of Labor Occupational Safety and Health Administration standards for daily occupational noise limits are specified in terms of the measurement based on A-weighting. The United States Environmental Protection Agency has selected A-weighting as the appropriate measure of environmental noise.

Considering that A-weighting comes from the listening experiment on pure tone, CCIR standardizes ITU-R 468 noise weighting for the measurement of random noise. It is most popular in Europe and former countries of the British Empire, such as Australia and South Africa. According to the ANSI standard [5], A-weighting frequency response can be calculated by (1) and (2):

$$R_a(f) = \frac{12200^2 f^4}{(f^2+20.6^2)(f^2+12200^2)(f^2+107.7^2)^{0.5}(f^2+737.9^2)^{0.5}}, \quad (1)$$

$$A = 2.0 + 20\log(R_a(f)). \quad (2)$$

The frequency response (amplitude) of ITU-R 468 noise weighting is shown in Fig. 2. A detailed table was provided in [6]. It differs greatly with A-weighting in the frequency range of 5 kHz to 8 kHz, where it peaks at 12.2 dB at 6.3 kHz.

To incorporate noise weighting into the ANC system, we derive digital filters approximating the magnitude responses shown in Fig. 2, as follows. First, a modified Yule-Walker method [19] is used to generate the infinite impulse response (IIR) filter. Since the resulting IIR filters do not fit the standard frequency responses in the low frequency range, a second-order Butterworth filter is cascaded to obtain the final IIR filters with acceptable fit to the curves shown in Fig. 2. We then obtain the desired finite impulse response (FIR) filter with an order of 100 by truncating the impulse responses of the resulting IIR filters. The energy of the truncated impulse response exceeds more than 99% of the energy of the initial impulse response. The FIR filter is chosen for noise weighting implementation because it is more tolerant of the quantization error in fixed-point implementation than the IIR filter. The result thus will be more meaningful for further realistic implementations.

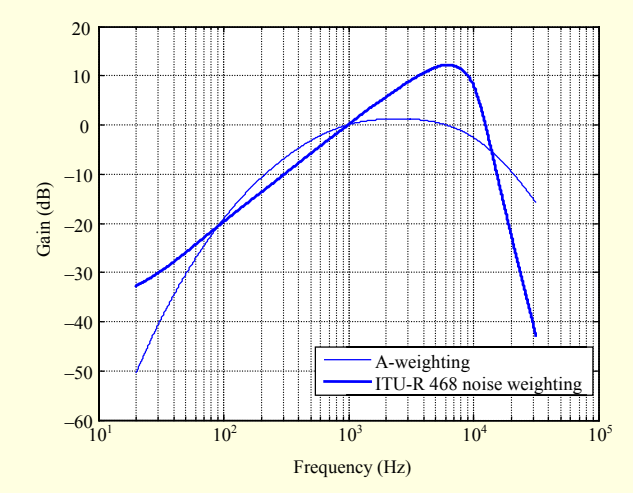

Fig. 2. Frequency responses of A-weighting (thin line) and ITU-R 468 noise weighting (bold line).

The frequency response (amplitude) of the designed filters with the Butterworth filter for A-weighting and ITU-R 468 noise weighting are displayed in Fig. 3. It is shown to be very close to the desired curve. FIR filters without Butterworth filters are also shown for comparison in Fig. 3.

3. PANC System with Noise Weighting

Figure 4 presents the PANC system based on the FELMS structure. The noise weighting filter, $H_{nw}(z)$, converts real residual noise $e(n)$ to pseudo residual noise $e_h(n)$, which is fed to the adaptive algorithm module. To make the system converge, a copy of $H_{nw}(z)$ is used following $\hat{S}(z)$. The NLMS method is adopted as the adaptive algorithm due to its simplicity and effectiveness.

The update equation of the adaptive filter can be expressed as

$$\mathbf{w}(n+1) = \mathbf{w}(n) + 2\mu e_h(n)\frac{\mathbf{x}_h(n)}{\mathbf{x}_h^T(n)\mathbf{x}_h(n)}, \quad (3)$$

where $\mathbf{w}(n) = [w_n(0), w_n(1), ..., w_n(L-1)]^T$ denotes the weight vector of the adaptive filter, L is the length of the adaptive filter, μ is the step size for the filter adaptation, $(\cdot)^T$ denotes the transpose operation, $e_h(n)$ is the output of filter $H_{nw}(z)$ with $e(n)$ as input, and $\mathbf{x}_h(n) = [x_h(n), x_h(n-1), ..., x_h(n-L+1)]^T$ is the output vector of the cascade filters $\hat{S}(z)$ and $H_{nw}(z)$ with $x(n)$ as the input. Noise weighting filter $H_{nw}(z)$ is designed as per the process described

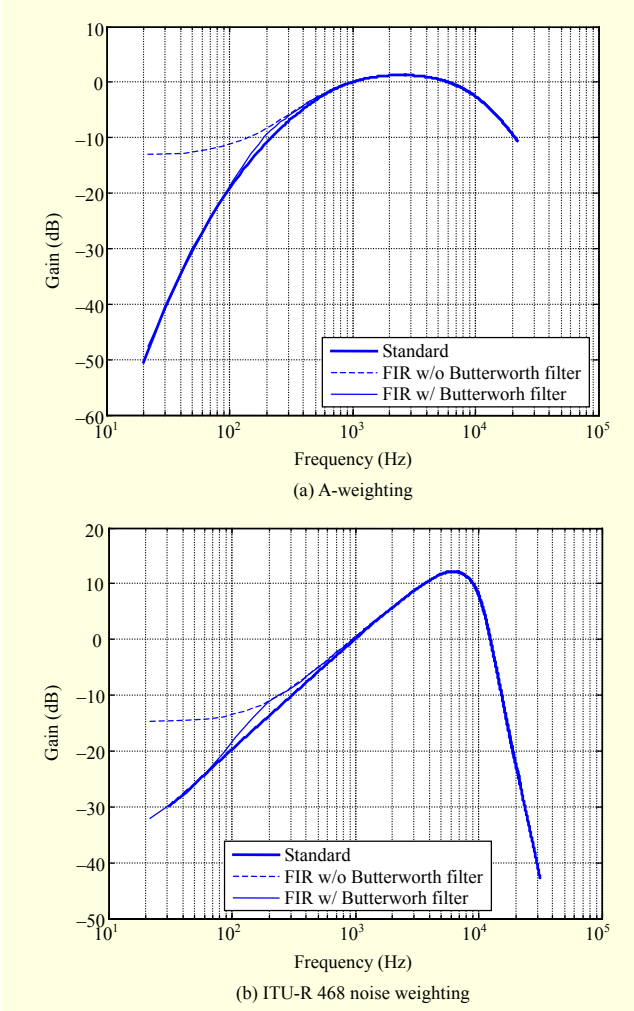

Fig. 3. Standard noise weighting curve (bold line) and designed FIR filter without (dashed line) and with (thin line) Butterworth filter compensation for (a) A-weighting and (b) ITU-R 468 noise weighting.

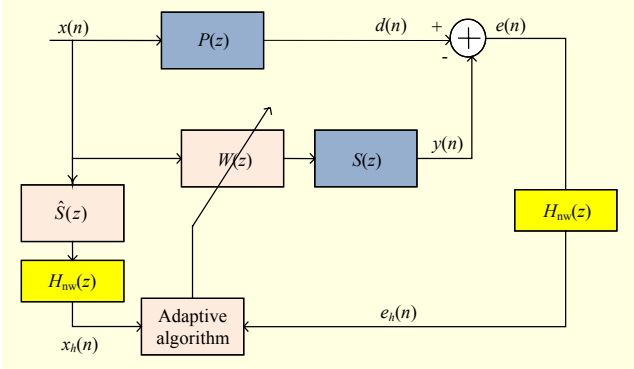

Fig. 4. PANC system with noise weighting based on FELMS structure.

in subsection II.2.

As shown in Fig. 4, the energy of pseudo residual noise $e_h(n)$ instead of that of real residual noise $e(n)$ is minimized. If we consider module $H_{nw}(z)$ as a model for the human ear, $e_h(n)$ is the perceived signal with $e(n)$ as the input signal to our hearing system. This means the energy of the perceived signal is minimized, which gives a quieter result in the perceptual sense than the conventional ANC system. Note that it is so far impossible to model the human ear perfectly. Since the noise weighting filter approximates the property of the human ear, $e_h(n)$ is closer to what we perceive than $e(n)$. Therefore, residual noise in the new system, shown in Fig. 4, is perceived to be quieter than that in the conventional system, shown in Fig. 1.

With respect to the computational complexity, the additional computation cost in this system compared to the conventional ANC system is the filtering operations for the noise weighting filter. The delay-less subband filtering scheme may be used to further reduce the computational burden [10].

III. Psychoacoustic Analysis

Psychoacoustics is the study of the human perception of sound. In this paper, we try to evaluate the ANC performance based on the human perception of residual noise. A subjective test is the most direct way to meet the goal. However, several drawbacks may restrict its usage: 1) inconsistent evaluation during testing, 2) disparage among listeners, 3) time cost for the testing setup and monetary cost for recruiting and training listeners, and 4) potential hearing damage during testing. Therefore, there is a need to apply an objective model to estimate the subjective evaluation. This section will describe the quantitative models for several psychoacoustic measurements.

1. Loudness

The perceptual intensity of a sound is modeled as loudness, which can be calculated as

$$L = \int_0^{24\,\text{Bark}} N' dz, \tag{4}$$

where L is the overall loudness and N' is the "specific loudness," that is, the loudness in a specific critical band in unit sone or unit Bark. Bark is the psychoacoustic scale for the critical band, which can be converted from the frequency in Hz as

$$\text{Bark} = 13\arctan(0.00076 f) + 3.5\arctan((f/7500)^2). \tag{5}$$

The calculation for specific loudness follows the standard ISO532B/DIN45631. The frequency masking effect is included in the loudness model. One sone is defined as the loudness of a 1-kHz tone with 40-dB SPL.

The process of calculating the specific loudness is as follows. The digitized signal is filtered with twenty-four 1/3 octave filters to decompose into critical bands. Then, the excitation level in each critical band is calculated with the decomposed signal. The specific loudness is then obtained with the excitation level, as described in [4].

2. Sharpness

The high frequency content of a sound is modeled as sharpness in the unit of acum. One acum is defined as the sharpness of a narrowband noise with one critical-band bandwidth at a center frequency of 1 kHz and a sound level of 60 dB.

It can be calculated as

$$S = 0.11 \frac{\int_0^{24\,\text{Bark}} N' g(z) z dz}{\int_0^{24\,\text{Bark}} N' dz} \text{ acum}, \quad (6)$$

where $g(z)$ is the weighting factor, which increases above 16 Bark to values larger than unity:

$$g(z) = \begin{cases} 1, & z \le 16, \\ 0.066 e^{0.171z}, & z > 16. \end{cases} \quad (7)$$

The sharpness sensation increases with frequency once it is greater than 16 Bark (about 3.15 kHz).

3. Roughness

The temporal variation of either amplitude or frequency is modeled as roughness in asper. One asper is the roughness of 60-dB, 1-kHz tone that is 100% modulated in amplitude at a modulation frequency of 70 Hz.

The frequency resolution and temporal resolution of the human hearing system determine the roughness of a sound. The frequency resolution can be represented by the excitation pattern or specific loudness versus critical-band rate pattern.

A quantitative model for roughness can be expressed as

$$R = 0.3 \frac{f_{\text{mod}}}{\text{kHz}} \int_0^{24\,\text{Bark}} \frac{\Delta L_{\text{E}}(z)}{\text{dB/Bark}} \text{ asper}, \quad (8)$$

where f_{mod} is the modulation frequency and $\Delta L_{\text{E}}(z)$ is the temporal masking depth in each critical band. $\Delta L_{\text{E}}(z)$ is further modeled by the ratio of maximum loudness and minimum loudness in each critical band.

4. Tonality

The tonal prominence of a sound is represented by tonality. There are several models of tonality. In this paper, we adopt the spectral flatness measure (SFM) [20] to quantify tonality. It measures the energy distribution among all spectral bands. High values indicate that the spectrum appears relatively flat and smooth. SFM is calculated by the ratio between the geometric mean of the power spectrum and the arithmetic mean of the power spectrum:

$$SFM = \frac{\sqrt[N]{\prod_{k=0}^{N-1} P(k)}}{\frac{1}{N}\sum_{k=0}^{N-1} P(k)}, \quad (9)$$

where $P(k)$ is the magnitude of the k-th DFT sample. Using SFM, tonality T is calculated by

$$SFM_{\text{dB}} = 10 \log_{10}(SFM), \quad (10)$$

$$T = \min\left(\frac{SFM_{\text{dB}}}{-60}, \ 1\right). \quad (11)$$

5. Pleasantness

The aforementioned psychoacoustic metrics measure four aspects of human hearing sensations. To measure the overall preferences by listeners, an integrated measurement of sound quality is required. In this paper, the sound quality is quantified by the empirical pleasantness model for pleasantness proposed in [13]:

$$P = e^{-0.55R} e^{-0.113S} (1.24 - e^{-2.2T}) e^{-(0.023L)^2}, \quad (12)$$

where R represents the roughness, S is the sharpness, T gives the value of tonality, L denotes the loudness, and P is the value of the overall pleasantness.

IV. Simulation and Discussion

Our simulations adopt two types of noise: synthetic random noise and realistic environmental noise. Modulated random noise is used as synthetic noise. MRI acoustic noise is chosen for realistic environmental noise. Some common configurations of two sets of simulations are described first. Primary and secondary path transfer functions $P(z)$ and $S(z)$ come from the measurements in our testbed, which mimics the MRI bore, as shown in Fig. 5. Two microphones are used to capture the input and output signals of the target acoustic path. Then, an adaptive FIR filter is used to model the impulse responses of the paths for $P(z)$ and $S(z)$. $P(z)$ and $S(z)$ are then truncated to a length of 100 each with the frequency response shown in Fig. 6 to simplify the simulation. Parameters are chosen as follows: sampling frequency is 44.1 kHz, adaptive filter uses NLMS algorithm, length of $W(z)$ is 1,000, and step size μ is empirically chosen as 0.05.

In each simulation, results of the following four cases are

Fig. 5. Testbed, which mimics the MRI bore for $P(z)$ and $S(z)$ measurements [16].

compared and analyzed.

- Case 1: ANC is off
- Case 2: Conventional ANC system
- Case 3: PANC system with A- weighting
- Case 4: PANC system with ITU-R 468 noise weighting.

1. Synthetic Random Noise

Random noise is chosen because it covers the full frequency band, which helps to give an overall evaluation of the human hearing sensation in the whole audible frequency range. Note that random noise shows very little roughness. To evaluate the effect on roughness, synthetic Gaussian white noise is amplitude-modulated with a modulation frequency of 70 Hz and modulation degree of 30%.

Simulations are conducted for the aforementioned four cases. Power spectrums of residual noises in Case 2, Case 3, and Case 4 are compared, as shown in Fig. 7. It can be seen that the incorporation of noise weighting in Case 3 and Case 4 changes the power spectrum of residual noise. The middle range (approximately 1 kHz to 12 kHz) is given more attenuation. The frequencies beyond this range are given less attenuation than that for Case 2. Furthermore, the incorporation of ITU-R 468 noise weighting in Case 4 causes greater weighting effect than the incorporation of A-weighting in Case 3.

Then, psychoacoustic analysis is done on the residual noises of these cases to quantify the perceptual effects of the above power spectrum changes. Figure 8 shows values of six metrics for each case: SPL, loudness, sharpness, roughness, tonality, and pleasantness. Psychoacoustic metric calculations are explained in section III. We specifically tabulate the comparison of Case 3 and Case 4 with Case 2 in Table 1. For SPL (dB), change C is calculated as

$$C = SPL_i - SPL_2 \quad (i = 3, 4). \tag{13}$$

For the other five metrics, change C is calculated in percentage as

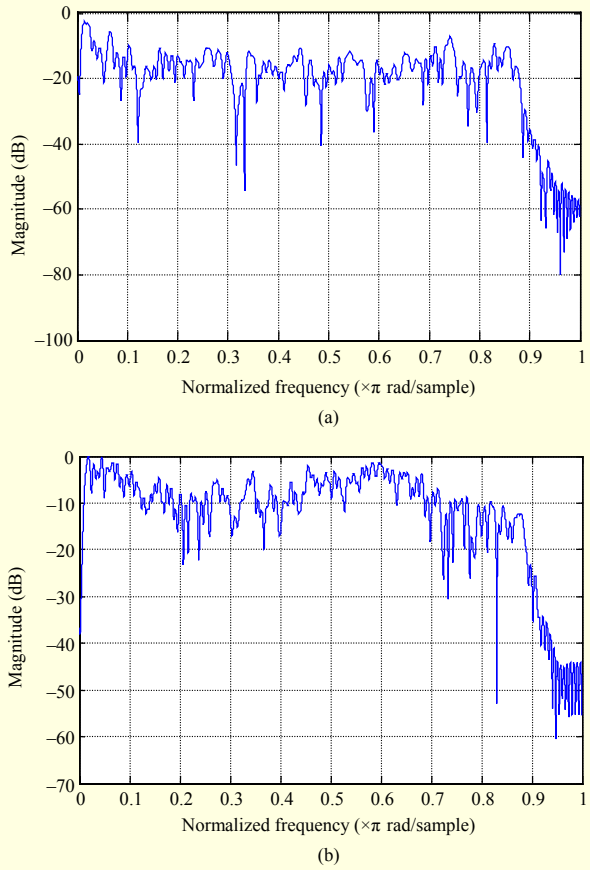

Fig. 6. Frequency response (magnitude) for (a) $P(z)$ and (b) $S(z)$ [16].

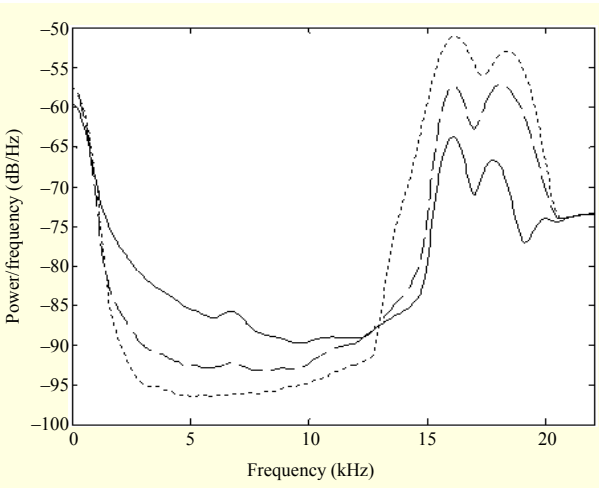

Fig. 7. Power spectrum comparison of residual noises in Case 2 (solid line), Case 3 (dashed line), and Case 4 (dotted line) with synthetic random noise as noise source.

$$C = \frac{M_i - M_2}{M_2} \times 100\% \quad (i = 3, 4), \tag{14}$$

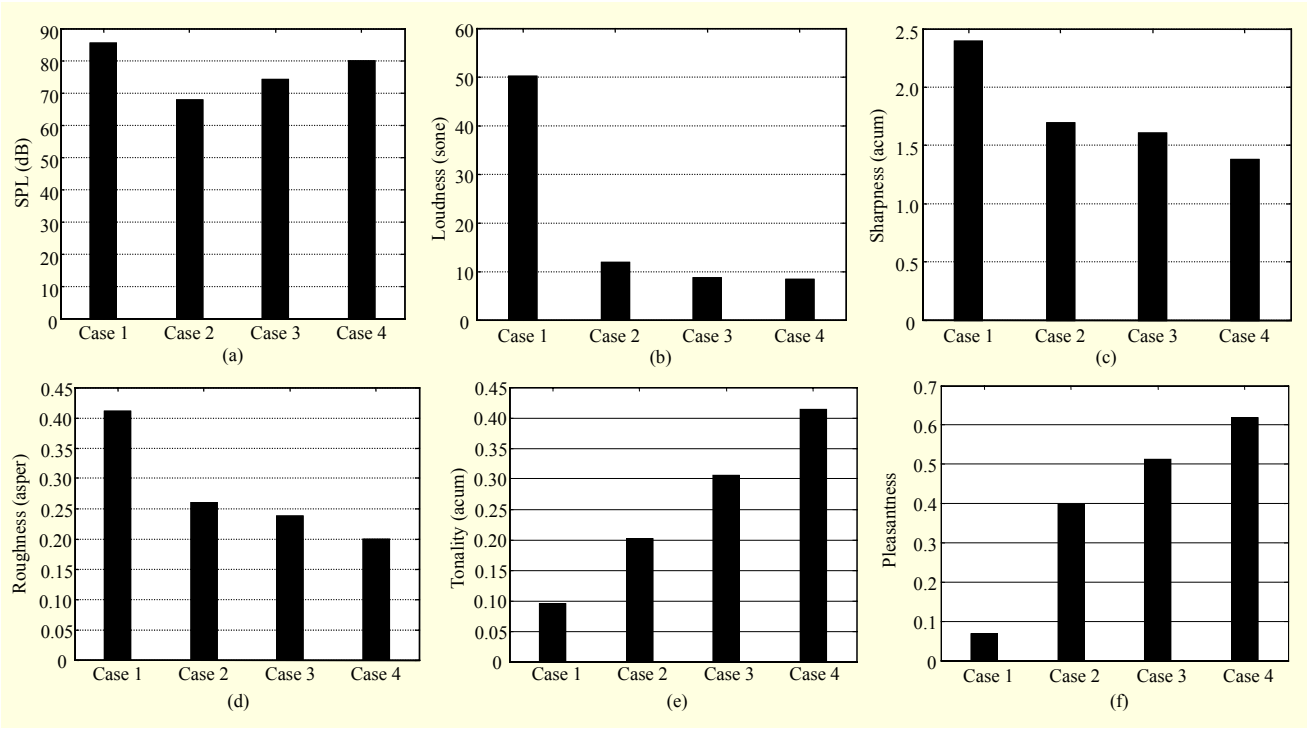

Fig. 8. Parameter analysis for synthetic random noises in four cases (Case 1: ANC is off; Case 2: conventional ANC; Case 3: PANC with A-weighting; Case 4: PANC with ITU-R 468 noise weighting): (a) SPL, (b) loudness, (c) sharpness, (d) roughness, (e) tonality, and (f) pleasantness.

Table 1. Residual noise change in Case 3 (PANC with A-weighting) and Case 4 (PANC with ITU-R 468 noise weighting) compared with Case 2 (conventional ANC) in terms of six metrics (SPL, loudness, sharpness, roughness, tonality, and pleasantness) with synthetic random noise as noise source.

	SPL	Loudness	Sharpness	Roughness	Tonality	Pleasantness
Case 3	6.35 dB	–26.76%	–5.19%	–8.54%	51.30%	28.96%
Case 4	12.17 dB	–30.65%	–18.61%	–22.90%	104.48%	55.58%

where M_i is the metric value for the i-th case.

It is interesting to see that we have higher SPL in Case 3 and Case 4 than in Case 2 (conventional ANC). However, the loudness values are reduced significantly, which are 26.76% and 30.65% for Case 3 and Case 4, respectively. It again demonstrates that the SPL is not positively proportional to human hearing perception. Sharpness values are reduced owing to the lower responses for high frequency components in noise weighting filters. Due to the nonuniform response in noise weighting, the spectrum flatness decreases in the PANC system, which increases the tonality values in Case 3 and Case 4. A roughness improvement may be explained in a way that the adaptive filter will attenuate a temporal change of loudness owing to the controller's adaptive nature. Overall, the pleasantness values are improved 28.96% and 55.58% in Case 3 and Case 4, respectively.

An informal listening test is used to order the four cases by their subjective pleasantness. Results show that Case 1 < Case 2 < Case 3 < Case 4, which verifies that the results by objective pleasantness model correlate with subjective sensation.

2. Realistic MRI Noise

Herein, we apply the new system to realistic MRI acoustic noise. As known, the rapid switching of the gradient coil in the MRI machine generates strong acoustic noise, which we refer to as scanner noise. The presence of scanner noise in the audible range not only creates a detrimentally annoying environment for patients and technicians but also interferes with functional MRI (fMRI) directly and indirectly [21], [22]. Direct interference comes with an increase in regional cerebral blood flow, interacting with the blood oxygen level dependent response of the brain activation. Indirect interference exists in the distraction on the perception of the stimulus by strong scanner noise. ANC technique has been applied to attenuate MRI scanner noise [23]. Perceptual improvement in the ANC system is especially meaningful to weaken the influence of acoustic scanner noise during fMRI examination.

In our experiment, MRI acoustic noise is recorded from a

Siemens 3-T Magnetom Trio. Diffuse-field microphones (B&K 2669C) and a data acquisition card (NI-PCI4472) are used for the recording. The noise is collected when the MRI machine is running echo planar imaging sequences at 16 slices per second. For the roughness calculation, we use 16 Hz as the modulation frequency. A power spectrum comparison for Case 2, Case 3, and Case 4 is shown in Fig. 9. Results of four cases in terms of six metrics are shown in Fig. 10. A quantitative comparison of Case 3 and Case 4 with Case 2 is shown in Table 2. It demonstrates again that incorporation of noise weighting increases the SPL but decreases the loudness values. Over that of Case 2, Case 3 and Case 4 show an improvement in pleasantness of 10.05% and 41.96%, respectively. To verify the improvement, we conduct an informal listening test. The preference in the informal test results is Case 1 < Case 2 < Case 3 < Case 4.

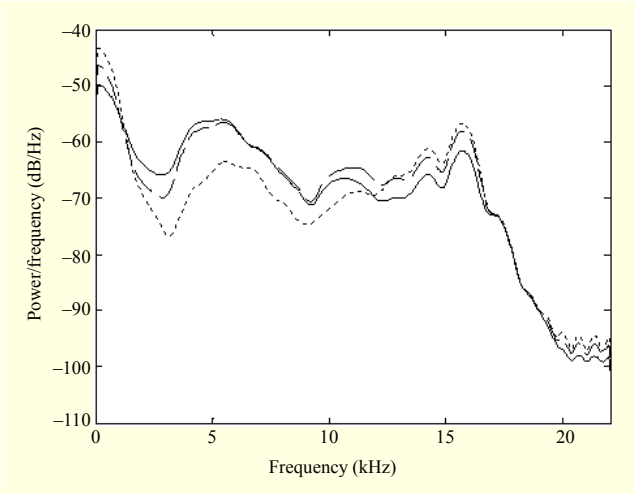

Fig. 9. Power spectrum comparison of residual noises in Case 2 (solid line), Case 3 (dashed line), and Case 4 (dotted line) with realistic MRI noise as noise source.

V. Conclusion

This paper proposed a method to improve ANC performance in terms of human hearing sensation. Noise weighting, instead

Table 2. Residual noise change in Case 3 (PANC with A-weighting) and Case 4 (PANC with ITU-R 468 noise weighting) compared with Case 2 (Conventional ANC) in terms of six metrics (SPL, loudness, sharpness, roughness, tonality, and pleasantness) with realistic MRI noise as noise source.

	SPL	Loudness	Sharpness	Roughness	Tonality	Pleasantness
Case 3	1.3 dB	–3.58%	1.25%	0.09%	10.50%	10.05%
Case 4	2.59 dB	–13.80%	–14.34%	1.79%	31.35%	41.96%

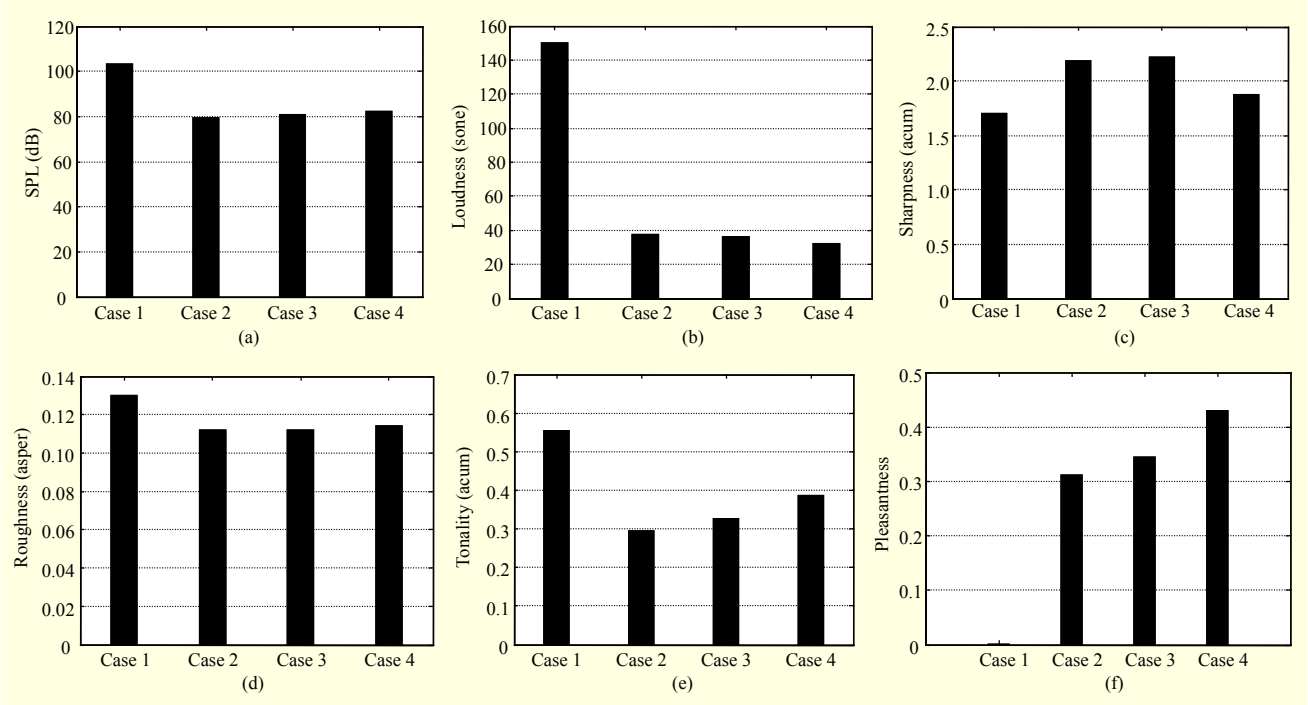

Fig. 10. Parameter analysis for realistic MRI acoustic noises in four cases (Case 1: ANC is off; Case 2: conventional ANC; Case 3: PANC with A-weighting; Case 4: PANC with ITU-R 468 noise weighting): (a) SPL, (b) loudness, (c) sharpness, (d) roughness, (e) tonality, and (f) pleasantness.

of a complicated nonlinear psychoacoustic model, was adopted to approximate the nonuniform property of human auditory system and incorporated into the ANC system based on the FELMS structure. Two popular standards, A-weighting and ITU-R 468 noise weighting, were used in the new system. These weightings were implemented as digital filters, which made it easy for a real-time system. Furthermore, we extended the evaluation tool from the commonly used SPL and previously used loudness in [8], [10] to sound quality, which tended to give an overall evaluation of sound in terms of pleasantness. An objective pleasantness model was used for this task. Both synthetic noise and realistic noise were taken for simulations. Results show that the new system improves not only loudness but also pleasantness, although SPL increases. Informal listening tests demonstrated that the results from the objective pleasantness model correlate with the subjective sensation. A comparison also indicated that a system with ITU-R 468 noise weighting performs better than one with A-weighting. This works as expected due to the difference in the nature of these two noise weightings. A-weighting is derived based on the measurement of tone signals. However, ITU-R 468 noise weighting is designed for wideband random noise. The fact that most of the realistic noises exhibited wideband characteristics makes the latter more suitable for practical use.

To verify the overall effect of noise weighting in the whole audible frequency range, we chose 44.1 kHz as the sampling frequency in our simulations. Some research claims that ANC is only effective for the low frequency domain. The small wavelength of a high frequency signal may limit the size of the quiet zone. In some ANC applications, the requirement for the quiet zone size is not strict because of the short distance between the speaker and human ear. However, it would still be helpful to test the proposed system for a low frequency noise signal in future work. Also, the dependence of the psychoacoustic performance on the nature of the noise source should be investigated.

References

[1] S.M. Kuo and D.R. Morgan, "Active Noise Control: A Tutorial Review," *Proc. IEEE*, vol. 87, no. 6, 1999, pp. 943-973.

[2] S. Haykin, *Adaptive filter theory*, 4th ed., Upper Saddle River, NJ: Prentice Hall, 2002.

[3] M.S. Sanders and E.J. McCormick, *Human Factors in Engineering and Design*, 7th ed., McGaw-Hill, 1993.

[4] H. Fastl and E. Zwicker, *Psychoacoustics: Facts and Models*, 3rd ed., Springer, 2006.

[5] ANSI, "American National Standard Specification for Sound Level Meters," ANSI S1.4-1983 (R2006), 2006.

[6] ITU, "Measurement of Audio-Frequency Noise Voltage Level in Sound Broadcasting," ITU-R Recommendation BS.468-4, 1986.

[7] S.M. Kuo and J. Tsai, "Residual Noise Shaping Technique for Active Noise Control Systems," *J. Acoustical Soc. America*, vol. 95, vol. 3, 1994, pp. 1665-1668.

[8] H. Bao and I. Panahi, "Using A-Weighting for Psychoacoustic Active Noise Control," *Proc. Int. Conf. IEEE Eng. Med. Biol. Soc.*, Vancouver, British Columbia, Canada, 2009, pp. 5701-5704.

[9] D.R. Morgan and J.C. Thi, "A Delayless Subband Adaptive Filter Architecture," *IEEE Trans. Signal Process.*, vol. 43, no. 8, 1995, pp. 1819-1830.

[10] H. Bao and I. Panahi, "Psychoacoustic Active Noise Control Based on Delayless Subband Adaptive Filtering," *Proc. IEEE Int. Conf. Acoust., Speech, Signal Process.*, Dallas, TX, USA, 2010, pp. 341-344.

[11] R. Guski, "Psychological Methods for Evaluating Sound Quality and Assessing Acoustic Information," *Acta Acustica United Acustica*, vol. 83, no. 5, 1997, pp. 765-774.

[12] H. Van der Auweraer, K. Wyckaert, and W. Hendricx, "From Sound Quality to the Engineering of Solutions for NVH Problems: Case Studies," *Acta Acustica United Acustica*, vol. 83, 1997, pp. 796-804.

[13] W. Aures, *Berechnungsverfahren für den Wohlklang beliebiger Schallsignale, ein Beitrag zur gehörbezogenen Schallanalyse*, PhD thesis, Munich University, 1984.

[14] M. de Diego et al., "Subjective Evaluation of Actively Controlled Interior Car Noise," *Proc. IEEE Int. Conf. Acoust., Speech, Signal Process.*, vol. 5, 2001, pp. 3225-3228.

[15] H. Bao et al., "Music Injection for Subjective Speech Enhancement and the Psychoacoustic Pleasantness Analysis," *Proc. Sensor, Signal Information Process. Workshop (SenSIP)*, Sedona, AZ, USA, May 2008.

[16] H. Bao and I. Panahi, "Psychoacoustic Active Noise Control with ITU-R 468 Noise Weighting and Its Sound Quality Analysis," *32nd Ann. Int. Conf. IEEE Eng. Med. Bio. Soc.*, 2010, pp. 4323-4326.

[17] H. Hassanpour and P. Davari, "An Efficient Online Secondary Path Estimation for Feedback Active Noise Control Systems," *Dig. Signal Process.*, vol. 19, no. 2, 2009, pp. 241-249.

[18] S.J. Elliott and P.A. Nelson, "Active Noise Control," *IEEE Signal Process. Mag.*, vol. 10, no. 4, 1993, pp. 12-35.

[19] B. Friedlander and B. Porat, "The Modified Yule-Walker Method of ARMA Spectral Estimation," *IEEE Trans. Aerosp. Electron. Syst.*, vol. AES-20, no. 2, 1984, pp. 158-173.

[20] ISO, "Information Technology – Multimedia Content Description Interface – Part4: Audio," ISO-IEC 15934-4 (E), 2001.

[21] A. Moelker and P.M.T. Pattynama, "Acoustic Noise Concerns in Functional Magnetic Resonance Imaging," *Human Brain Mapping*, vol. 20, no. 3, 2003, pp. 123-141.

[22] D. Tomasi et al., "fMRI-Acoustic Noise Alters Brain Activation

During Working Memory Tasks," *NeuroImage*, vol. 27, no. 2, 2005, pp. 377-386.
[23] J. Chambers et al., "Developments in Active Noise Control Sound Systems for Magnetic Resonance Imaging," *Appl. Acoustics*, vol. 68, no. 3, 2007, pp. 281-295.

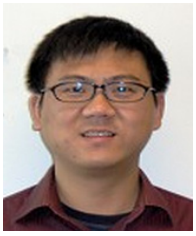

Hua Bao received his Ph.D. from the Department of Electrical Engineering at the University of Texas at Dallas, TX, USA, in 2010. He is currently working as a senior staff scientist at the Mobile and Wireless Group of Broadcom Corporation, NJ, USA. His research is in the area of digital signal processing for audio and speech signals, including active noise control, dereverberation, speech enhancement, and corresponding system design on integrated circuit.

Issa M.S. Panahi received his Ph.D. degree in electrical engineering from the University of Colorado at Boulder in 1988. He joined the faculty of the University of Texas at Dallas (UTD), TX, USA, after working in the industry for 15 years. Dr. Panahi is now an associate professor in the Department of Electrical Engineering at UTD. He is the director of the Statistical Signal Processing and Acoustic Research Laboratories at UTD. His research areas include MIMO digital signal processing, source separation, signal estimation, system identification, noise cancellation, speech enhancement, acoustics, and embedded DSP systems. From 1988 to 1991, he was a research scientist in the Geophysical Signal Processing Group at Bellaire Research Lab, Shell Oil Development, Houston, TX, USA. From 1991 to 2000, he worked as the DSP chief architect, a worldwide applications manager, a senior member of the technical staff, the chief technology officer, and an advance systems development manager in the embedded DSP systems business unit at Texas Instruments, Inc., in Houston, TX, USA. He was an application manager with the Wireless/OMAP Group, Texas Instruments, Dallas, TX, USA, before joining UTD in 2001. He holds one US patent. He is the author or coauthor of several Texas Instruments books and has authored over 70 published conference, journal, and technical papers.